Analytical Methods

International Edition: DOI: 10.1002/anie.201502171
German Edition: DOI: 10.1002/ange.201502171

Reliable Quantitative SERS Analysis Facilitated by Core–Shell Nanoparticles with Embedded Internal Standards**

*Wei Shen, Xuan Lin, Chaoyang Jiang, Chaoyu Li, Haixin Lin, Jingtao Huang, Shuo Wang, Guokun Liu, Xiaomei Yan, Qiling Zhong, and Bin Ren**

Abstract: *Quantitative analysis is a great challenge in surface-enhanced Raman scattering (SERS). Core-molecule-shell nanoparticles with two components in the molecular layer, a framework molecule to form the shell, and a probe molecule as a Raman internal standard, were rationally designed for quantitative SERS analysis. The signal of the embedded Raman probe provides effective feedback to correct the fluctuation of samples and measuring conditions. Meanwhile, target molecules with different affinities can be adsorbed onto the shell. The quantitative analysis of target molecules over a large concentration range has been demonstrated with a linear response of the relative SERS intensity versus the surface coverage, which has not been achieved by conventional SERS methods.*

Surface-enhanced Raman spectroscopy (SERS) can provide fingerprint information of target molecules and has been considered to be an ultrasensitive label-free detection method for a variety of applications.[1] However, it is still a great challenge to use SERS as a quantitative technique because SERS is inherently a near-field phenomenon and only those molecules located (usually <2 nm) within the highly enhanced electromagnetic field (so called hot spot) make a significant contribution to the overall SERS signal. Furthermore, the field enhancement in the hot spots is sensitive to the detailed local structure as well as the coupling between nanostructures, and can vary by several orders of magnitude.[2] Therefore, even if the molecules can be uniformly distributed on the metal surfaces, the SERS signals may still be non-uniform. The merits of the high molecular sensitivity and the difficulties to realize quantitative analysis both contribute to the vibrant quantitative SERS analysis.[1f]

Quantitative SERS analysis can be divided into two categories: solid substrate based analysis and nanoparticle sol-based analysis.[3] In both categories, the key issue is to fabricate SERS-active materials and control the uniformity of the hot spots. Sensitivity and reproducibility are two irreconcilable parameters in the solid substrate based analysis and there is still no ideal substrate that can at the same time achieve both properties.[3,4] The use of an internal standard (IS) has been proposed to overcome the above-mentioned problems.[3,5] However, the requirement of locating the IS and target molecules in the same physical and chemical environment is a nontrivial issue since the SERS measurements are conducted with a multiphase system and SERS intensity depends on the highly localized near-field enhancement. Even in an ideal case that the IS and target molecules can be uniformly dispersed on the SERS-active surface in an indiscriminate microenvironment, there are still some problems: 1) the IS molecules will compete for the surface adsorption site and replacement may occur, and 2) the IS signal may be influenced by the microenvironment, thereby leading to a change in the intensity and frequency.[1f,3,6] The use of structural analogues of target molecules as internal standards may partially overcome the problems. However, it still cannot solve the problem of dynamic exchange and competitive adsorption when their concentrations are significantly different. It is highly desirable to develop a novel type of IS whose SERS signals will not be influenced by the external environment for a broad range of SERS analyses.

Recently, there has been increasing interest in synthesizing SERS-active core-molecule-shell nanoparticles (CMS NPs), in which a molecular layer is sandwiched between the core and shell of noble metals.[7] CMS NPs have exhibited stable and strong SERS signals and have been used as SERS tags for indirect analyses and imaging. In fact, CMS NPs might be an ideal IS material for quantitative SERS analysis, since: 1) the molecular layer is sandwiched between the core and shell, and will not be influenced by the outer environment; 2) the shell surface is totally free and can be accessed by target molecules without worrying about dynamic replacement; 3) the nanoparticle is simultaneously used as an internal standard and enhancing substrate, without affecting the spatial distribution of target molecules; and 4) it is a label-free technique and the signal is from the target molecules adsorbed on the open shell surface. To date, there has been no

[*] W. Shen, C. Y. Li, H. X. Lin, J. T. Huang, S. Wang, Dr. G. K. Liu, Prof. X. M. Yan, Prof. B. Ren
State Key Laboratory of Physical Chemistry of Solid Surfaces
Collaborative Innovation Center of Chemistry for Energy Materials (iChEM), MOE laboratory of Spectrochemical Analysis and Instrumentation, The Key Laboratory for Chemical Biology of Fujian Province, College of Chemistry and Chemical Engineering
Xiamen University, Xiamen 361005 (China)
E-mail: bren@xmu.edu.cn
Homepage: http://bren.xmu.edu.cn
X. Lin, Prof. Q. L. Zhong
College of Chemistry and Chemical Engineering
Jiangxi Normal University, Nanchang 330022 (China)
Prof. C. Y. Jiang
Department of Chemistry, The University of South Dakota
414 E. Clark St., Vermillion, SD 57069 (USA)

[**] We acknowledge support from MOST (2011YQ03012400 and 2013CB933703), NSFC (21227004, 21321062, 21473140, and J1310024), and MOE (IRT13036). C.J. thanks the PCOSS Fellowship program for support. SERS = surface-enhanced Raman scattering.
Supporting information for this article is available on the WWW under http://dx.doi.org/10.1002/anie.201502171.

report of this type of approach for direct quantitative SERS analysis.

A common practice for coating a complete metal shell over a molecule-coated nanoparticle core is to use a molecule with bifunctional groups to simultaneously bind to the core metal surface and capture the metal ions for shell formation.[7] Bifunctional molecules, such as DNA, 4-mercaptobenzoic acid (MBA), and 1,4-benzenedithiol, have been used as the linkers to prepare CMS NPs that act as SERS tags.[7] These molecules serve as both the linker and the Raman tag that should produce a strong SERS signal. Such a requirement limits, to some extent, the range of molecules that can be used. Herein, we modified the existing method by replacing the previous single component molecular layer with two components: one with a strong Raman signal to act as the SERS IS, and another molecule as a framework to form the shell. Such a modification would significantly expand the range of SERS internal standards. We convincingly demonstrate that the CMS NPs are highly suitable for the quantitative SERS analysis of different types of samples with a much improved dynamic range, reproducibility, and reliability. This method is versatile and sensitive and provides an immediate solution to the bottle-neck problem in the label-free detections with ultrahigh sensitivity.

The synthesis of the CMS NPs with two types of embedded molecules is shown in Figure 1 a (the synthetic details are given in the Supporting Information; see section S1.2). We chose gold nanospheres as the core to obtain a highly uniform core, silver as the shell to achieve the highest possible enhancement, cysteamine (CA) as the framework, and 4-mercaptopyridine (Mpy) as the Raman probe. Both CA and Mpy can bind to the gold cores through Au–S bonds and the silver atoms can be easily deposited on the CA layer as a result of the strong affinity of the amino group. The transmission electron microscopy (TEM) images (Figure 1 b) of the CMS NPs indicate that the CMS NPs are structurally uniform and a light silver shell surrounding the dark gold core can be clearly identified. The average diameter of the CMS NPs is about 60.2 ± 3.0 nm (see Figure S1 and Table S1), which is larger than that of gold nanospheres (50.2 ± 1.8 nm). The narrow size distribution of the CMS NPs and their high dispersibility were further confirmed by high-sensitivity flow cytometry measurements (Figure S2 and Table S2).[8] The best way to demonstrate the core–shell structure was to perform scanning TEM (STEM) measurements to obtain the spatial distribution of the Au core, the Ag shell, and the embedded molecular layer (Figure 1 c). The STEM images of Au and S are very similar, thus indicating that the S takes the shape of the Au nanosphere. The superimposed STEM image of Ag and S (Figure 1 d) clearly shows that the molecular layer retains its integrity and the molecules do not spill out to the surface of the silver shell. All these observations indicate that we had successfully obtained the designed CMS nanostructures.

The optical properties of the CMS NPs, revealed by UV/Vis spectroscopy and SERS tests, indicate that these nanoparticles are ideal substrates and internal standards for SERS study. The CMS NPs have a strong localized surface plasmon resonance at approximately 520 nm and a broad shoulder

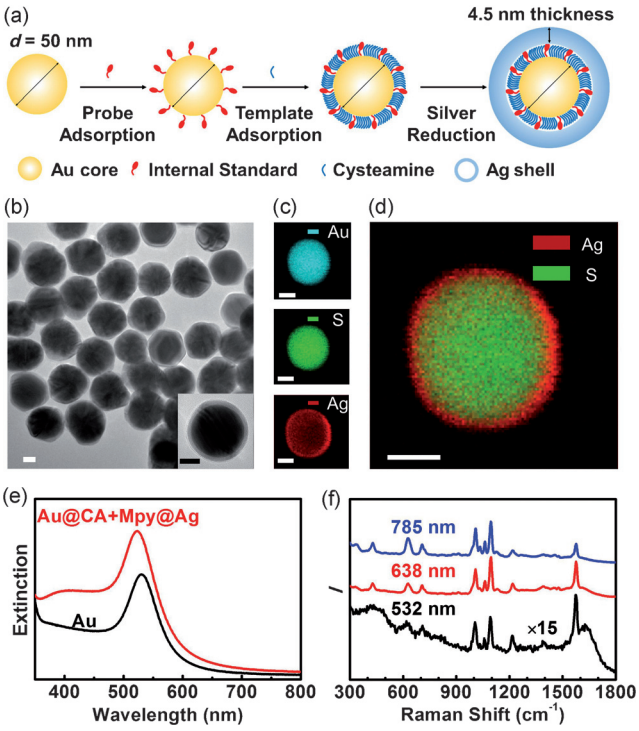

Figure 1. Synthesis and characterization of the molecular monolayer embedded between the Au core and Ag shell. a) Synthetic scheme for the Au@CA + Mpy@Ag NPs (CMS NPs). b) TEM images of the CMS NPs. c) STEM images of the CMS NPs using the Au-M, S-K, and Ag-L signals. d) The superimposed image of the STEM images of Ag-L and S-K. e) UV/Vis spectra of the Au NPs and CMS NPs. f) SERS spectra of the CMS NP colloids at different wavelengths. All the scale bars are 20 nm. Each spectrum was the mean of five spectra and the collection time was 10 s.

around 400 nm (Figure 1 e and Figure S3). The SERS spectra of the CMS NPs (M = CA + Mpy) excited using three lasers (Figure 1 f) all have a Mpy Raman band at 1575 cm^{-1}, which implies that the Mpy molecules are linked between the core and the outer shells in a double-linkage mode.[9] The SERS signals come from individual CMS NPs in the colloidal solution (see sections S2.4–S2.7). The SERS signals observed under laser excitation at 638 or 785 nm are much stronger than that at 532 nm. We attempted to use the finite difference time domain (FDTD) method to simulate the near-field electromagnetic field of the CMS NPs. However, the simulation results cannot so far explain the experimental ones. This discrepancy may be due to the complicated coupling of the molecule with the strong electromagnetic field in the closed small cavity, which is worthy of further theoretical studies. Nonetheless, sufficient SERS signals can be obtained from the CMS NPs with excitation at either 638 or 785 nm, which allows their convenient utilization as internal standards for quantitative SERS analyses.

The applicability of the CMS NPs for quantitative SERS analysis was demonstrated by using 1,4-phenylene diisocyanide (PDI) as a target, since PDI has a unique isocyanide band at about 2200 cm^{-1}, has no fluorescent background, and can effectively induce aggregation of the NPs for a strong SERS response. As a consequence of the dynamic nature of

the NP aggregation process, we acquired time-dependent SERS signals after addition of PDI (5×10^{-7} M) to determine the experimental parameters required to obtain a stable SERS signal. After addition of PDI, we observed an abrupt increase in the Mpy signal and a slow increase in the PDI signal with extended incubation time (Figure 2a and see

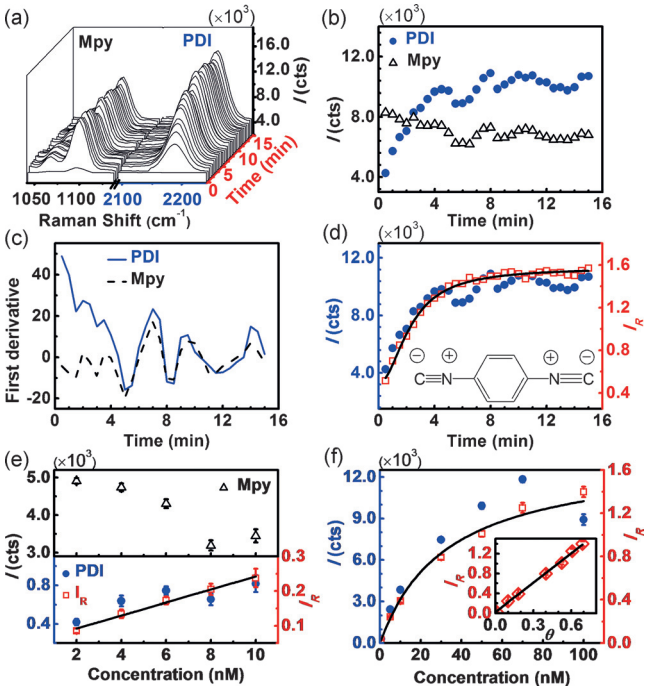

Figure 2. SERS monitoring of the aggregation process after addition of target molecules (PDI) and the working curves in the quantitative SERS analysis. a) Time-dependent SERS spectra of Mpy (internal standard, IS) and PDI (target). b) The SERS intensities of the target and IS fluctuate with the incubation time. c) The first derivative of the intensities of the IS and target. d) Time-dependent SERS intensity of the target and the intensity ratio of the target to IS. e) A plot of the SERS intensities of the internal standard (Mpy, open triangle), target (PDI, solid circle), and relative intensities (open square) at various PDI concentrations. f) A plot of the SERS intensities and the relative ones versus the PDI concentration over a large concentration range; the inset is a plot of the relative intensities against the PDI surface coverage. The laser power was 3.4 mW in the kinetic study (a–d) and 6.6 mW for quantitative analyses (e,f). The collection time was 25 s for (a–d) and 10 s for (e,f). Each point in (e) and (f) is the mean of 16 spectra.

Figure S7 for the full range). PDI molecules can induce rapid aggregation of the CMS NPs, which leads to an abrupt increase in the Mpy signal, and the remaining PDI in solution may slowly diffuse into the hot spots. Both SERS signals still fluctuate even after 10 min (Figure 2b and Figure S8a). The dynamic light scattering (DLS) results show that aggregates were formed in the solution with a size of 350 to 800 nm (Figure S9a), and the inhomogeneous aggregates precipitated (Figure S9b). All these, together with the dynamic nature of the CMS NP aggregates, will contribute to the fluctuation of the SERS intensities.

Very interestingly, the PDI signal fluctuates synchronously with that of Mpy, as shown in the first derivative analysis of the SERS intensities (Figure 2c). It is clear that such an accompanying fluctuation may have the same origin, possibly from the inhomogeneous aggregates in the colloid. Therefore, normalizing the PDI signal (2184 cm^{-1}) to that of Mpy (using the band at 1095 cm^{-1}) may correct the fluctuations in both the aggregation state of the nanoparticles and the instrumental factors. Indeed, we found that the relative SERS intensity of PDI to Mpy becomes more stable after 10 min (Figure 2d and Figure S8b) compared with the absolute SERS intensity of PDI. Furthermore, a better data reproducibility of less than 8% relative standard deviation was achieved between batches after correction using the internal standards. Hence, an incubation of 10 min was used for the rest of the quantitative SERS analyses.

We used PDI (target) solutions with different concentrations to demonstrate the applicability of the CMS NPs for quantitative SERS analysis. The SERS intensity of PDI fluctuates at different PDI concentrations (Figure 2e, solid circle). These raw data give a poor linear response, which is reasonable considering the inhomogeneous aggregation of NPs and the possible precipitation of large aggregates, as reflected by the SERS intensity of Mpy (IS; Figure 2e top panel, open triangle). The linearity of the working curve can be improved by normalizing the data to the SERS intensities of Mpy (Figure 2e, open square). Clearly, the SERS signals of Mpy give an effective feedback and the Mpy plays the role of an ideal IS for quantitative SERS analysis. One can further improve the batch-to-batch slope reproducibility by controlling the amount of remaining citrate ions in the solution (see section S3.3). The accuracy of the working curve was then checked by using a 5 nM PDI solution. The testing point is located on the working curve with an error of 1.2%, which is far better than the accuracy required for trace analysis (Figure S10d). The data normalized to an Mpy IS gives better and more reproducible limits of detection (LOD) compared with those without normalization (Figure S11).

Another challenge for quantitative SERS analysis is whether the method can be extended to a larger range of analyte concentrations. For this purpose, the working curve for PDI concentrations from 0.5 nM to 100 nM was measured (Figure 2f). The abrupt weak SERS signal for PDI at 100 nM is due to severe precipitation of the CMS NPs at a high PDI concentration (agreeing with the UV/Vis data, Figure S9b). After normalization with the IS, the working curve becomes smooth and can be perfectly fitted to Langmuir adsorption behavior with an equilibrium constant (K_T) of 2.2×10^7 nM^{-1}.[6c] Furthermore, the relative standard deviation of K_T can be significantly improved (from 45% to 12%) by normalization. From the obtained K_T value, we can calculate the surface coverage of PDI molecules at different concentrations. Surprisingly, we found a very good linear increase in the relative PDI SERS intensity with the increasing PDI surface coverage (inset of Figure 2f). Such linearity over a large concentration range is the basis of the quantitative SERS analysis. Up to now, we have not found any report discussing such a linear relationship in SERS (see section S3.5).

We also applied the CMS NPs to the quantitative SERS analysis of other target molecules with less affinity to the

SERS substrates. For example, basic red 9 (BR9) is a forbidden dye in the textile industry and has a weak affinity to silver. Figure 3a shows the SERS spectra of BR9 on the CMS NPs; the band at 825 cm^{-1} was used for quantitative analysis.

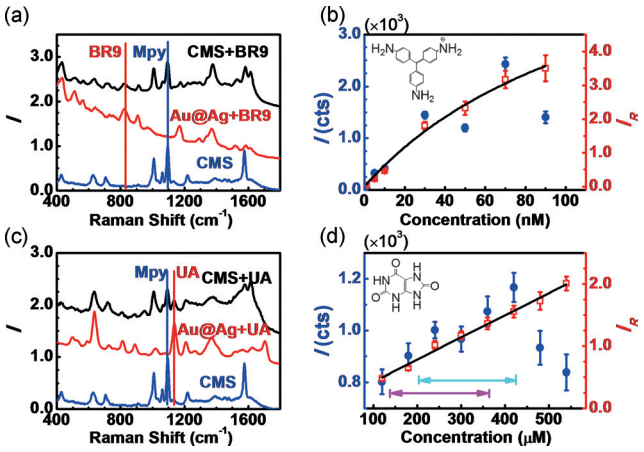

Figure 3. a) SERS spectra to identify the fingerprints of BR9 (825 cm^{-1}, 50 μM BR9 for Au@Ag NPs, and 5 nM BR9 for CMS NPs). b) A plot of the BR9 SERS intensities (solid circle) and relative ones (open square) at various BR9 concentrations. c) SERS spectra to identify the fingerprints of UA (1135 cm^{-1}, 800 μM UA for Au@Ag NPs, and 130 μM UA for CMS NPs). d) A plot of the UA SERS intensities (solid circle) and relative ones (open square) at various UA concentrations; the turquoise region indicates the range of UA concentration in the blood of a normal male; the purple region is that of a normal female). The laser power was 6.6 mW (638 nm). Each point is the mean of 16 spectra and the collection time for each spectrum was 10 s.

The relative SERS intensities of BR9 follow a very nice Langmuir-type curve over a broad concentration range of 0.5 nM to 100 nM (Figure 3b). Such a low LOD is hard to achieve in traditional SERS analysis because of the competitive adsorption of internal standards. Sensitive quantitative analysis of weakly adsorbed molecules is essential for applications such as environmental monitoring, food testing, as well as in situ and in vivo detection.

We further applied the CMS NPs to the quantitative SERS analysis of molecules, such as uric acid (UA), that have much weaker SERS intensities as a result of their small Raman cross-sections. UA is a common final metabolite of purine-related species in human blood, with a concentration range of 200–430 μM for males and 140–360 μM for females. Abnormal concentrations of UA are usually associated with some diseases and should be carefully monitored. UA produces a band at 1135 cm^{-1} (Figure 3c), which is strong enough for detailed analyses. A linear response of the relative SERS intensity of UA to Mpy versus the UA concentration was obtained (Figure 3d). The linear working curve covers the concentration range of normal humans, which is sufficient to provide quantitative data for diagnoses in a fast and inexpensive manner. A further development will be to design more sophisticate CMS NPs that will not only have enough sensitivity to quantitatively detect the UA in human blood, but also possess necessary selectivity that can deal with the complicated samples with less steps of purifications and separations.

In contrast to the reported CMS studies, the introduction of a framework layer of CA makes the present method more versatile and suitable for preparing SERS-active core–shell nanoparticles with different IS molecules to avoid spectral overlap with the analytes. For example, we have synthesized CMS NPs containing MBA or thiophenol with similar SERS properties to Au@CA + Mpy@Ag (Figure S12a–c) for quantitative SERS analysis of PDI (Figure S12d). On the other hand, using other types of sandwich structures, such as Ag@M@Ag and Ag@M@Au, as well as other shapes of core and/or shells, may also be possible. We are currently investigating such modifications with the aim of developing some new types of functional nanoparticles and expanding the SERS application.

In summary, we have developed a novel quantitative SERS method based on core-molecule-shell nanoparticles. The two components in the molecular layer play different roles: one helps to form the shell and the other gives a strong Raman signal and is used as the internal standard (IS). Since the IS is embedded inside the shell and the target molecule is adsorbed on the shell surface, they will not compete for the surface sites, and the IS signal will not be influenced by the detection environment. Our results convincingly demonstrate that the IS signal can effectively correct the signal fluctuation as a result of the different aggregation states and measuring conditions, which allows a reliable quantitative SERS analysis of targets with different affinities to the surface. The flexibility in choosing the Raman probe, the core, and shell materials (materials, size, and shape) will make this method applicable for the quantitative SERS detection of a wide variety of targets.

Keywords: analytical methods · internal standards · nanoparticles · quantitative analysis · Raman spectroscopy

How to cite: *Angew. Chem. Int. Ed.* **2015**, *54*, 7308–7312
Angew. Chem. **2015**, *127*, 7416–7420

[1] a) S. Nie, S. R. Emory, *Science* **1997**, *275*, 1102–1106; b) K. Kneipp, Y. Wang, H. Kneipp, L. T. Perelman, I. Itzkan, R. R. Dasari, M. S. Feld, *Phys. Rev. Lett.* **1997**, *78*, 1667–1670; c) J. F. Li, Y. F. Huang, Y. Ding, Z. L. Yang, S. B. Li, X. S. Zhou, F. R. Fan, W. Zhang, Z. Y. Zhou, D. Y. Wu, B. Ren, Z. L. Wang, Z. Q. Tian, *Nature* **2010**, *464*, 392–395; d) D. Cialla, A. März, R. Böhme, F. Theil, K. Weber, M. Schmitt, J. Popp, *Anal. Bioanal. Chem.* **2012**, *403*, 27–54; e) M. Moskovits, *Phys. Chem. Chem. Phys.* **2013**, *15*, 5301–5311; f) S. Schlücker, *Angew. Chem. Int. Ed.* **2014**, *53*, 4756–4795; *Angew. Chem.* **2014**, *126*, 4852–4894.

[2] a) S. M. Stranahan, K. A. Willets, *Nano Lett.* **2010**, *10*, 3777–3784; b) H. Xu, E. J. Bjerneld, M. Käll, L. Börjesson, *Phys. Rev. Lett.* **1999**, *83*, 4357–4360.

[3] S. E. J. Bell, N. M. S. Sirimuthu, *Chem. Soc. Rev.* **2008**, *37*, 1012–1024.

[4] a) M. J. Natan, *Faraday Discuss.* **2006**, *132*, 321–328; b) Y. Fang, N.-H. Seong, D. D. Dlott, *Science* **2008**, *321*, 388–392; c) M. C. S. Pierre, P. M. Mackie, M. Roca, A. J. Haes, *J. Phys. Chem. C* **2011**, *115*, 18511–18517; d) B. L. Darby, E. C. Le Ru, *J. Am. Chem. Soc.* **2014**, *136*, 10965–10973.

[5] a) L. Chen, J. Choo, *Electrophoresis* **2008**, *29*, 1815–1828; b) Y. Yin, T. Qiu, W. Zhang, P. K. Chu, *J. Mater. Res.* **2011**, *26*, 170–185;

c) E. Kämmer, K. Olschewski, T. Bocklitz, P. Rösch, K. Weber, D. Cialla, J. Popp, *Phys. Chem. Chem. Phys.* **2014**, *16*, 9056 – 9063.
[6] a) C. Caro, C. López-Cartes, P. Zaderenko, J. A. Mejías, *J. Raman Spectrosc.* **2008**, *39*, 1162 – 1169; b) S. M. Ansar, X. Li, S. Zou, D. Zhang, *J. Phys. Chem. Lett.* **2012**, *3*, 560 – 565; c) S. Kasera, F. Biedermann, J. J. Baumberg, O. A. Scherman, S. Mahajan, *Nano Lett.* **2012**, *12*, 5924 – 5928.
[7] a) Y. Feng, Y. Wang, H. Wang, T. Chen, Y. Y. Tay, L. Yao, Q. Yan, S. Li, H. Chen, *Small* **2012**, *8*, 246 – 251; b) D.-K. Lim, K.-S. Jeon, J.-H. Hwang, H. Kim, S. Kwon, Y. D. Suh, J.-M. Nam, *Nat. Nanotechnol.* **2011**, *6*, 452 – 460; c) N. Gandra, S. Singamaneni, *Adv. Mater.* **2013**, *25*, 1022 – 1027; d) J. Song, B. Duan, C. Wang, J. Zhou, L. Pu, Z. Fang, P. Wang, T. T. Lim, H. Duan, *J. Am. Chem. Soc.* **2014**, *136*, 6838 – 6841.
[8] S. Zhu, L. Yang, Y. Long, M. Gao, T. Huang, W. Hang, X. Yan, *J. Am. Chem. Soc.* **2010**, *132*, 12176 – 12178.
[9] X.-S. Zheng, P. Hu, J.-H. Zhong, C. Zong, X. Wang, B.-J. Liu, B. Ren, *J. Phys. Chem. C* **2014**, *118*, 3750 – 3757.

Received: March 7, 2015
Published online: May 4, 2015

